antibiotics

MDPI

Article

In silico screen identifies a new family of agonists for the bacterial mechanosensitive channel MscL

Robin Wray [1], Paul Blount [1,*], Junmei Wang [2,*] and Irene Iscla [1,*]

[1] Department of Physiology, UT Southwestern Medical Center, 5323 Harry Hines Blvd, Dallas, TX, 75390-9040

[2] Department of Pharmaceutical Sciences and Computational Chemical Genomics Screening Center, University of Pittsburgh School of Pharmacy, Pittsburg, PA, 15261

* Correspondence: II: Irene.Iscla@gmail.com; JW: junmei.wang@pitt.edu; PB: Paul.Blount@utsouthwestern.edu

Abstract: MscL is a highly conserved mechanosensitive channel found in the majority of bacterial species, including pathogens. It functions as a biological emergency release valve, jettisoning solutes from the cytoplasm upon acute hypoosmotic stress. It opens the largest gated pore known and has been heralded as an antibacterial target. Though there are no known endogenous ligands, small compounds have recently been shown to specifically bind to and open the channel, leading to decreased cell growth and viability. Their binding site is at the cytoplasmic/membrane and subunit interfaces of the protein, which has been recently been proposed to play an essential role for channel gating. Here we have targeted this pocket using *in silico* screening, resulting in the discovery of a new family of compounds, distinct from other known MscL-specific agonists. Our findings extend the study of this functional region, the progression of MscL as a viable drug target, and demonstrate the power of *in silico* screening for identifying and improving the design of MscL agonists.

Keywords: : Bacterial channels, antibiotic resistance, bacterial drug target

1. Introduction

The mechanosensitive channel of large conductance, MscL, is a homopentameric protein found in the cytoplasmic membrane of the vast majority of bacterial species, as well as some fungi [1-3]. It serves as a biological emergency release valve, gated by membrane tension effected by the sudden decrease in the osmolarity of the environment [2-4]. The opening of MscL's huge pore, on the order of 25 to 30Å [5,6], allows osmoprotectants, that are accumulated or synthesized at higher osmolarity, to rapidly jettison from the cell, avoiding lyses and thus reaching osmotic homeostasis [3,7]. Not surprisingly, inappropriate gating of the MscL channel, either by mutations [8-11] or post-translational modifications [9], is detrimental to the cell, causing the channel to leak valuable metabolites, which leads to slowed growth and decreased viability.

These finding suggested that MscL could be a viable novel drug target for difficult-to-treat bacterial infections. Indeed, one study independently identified MscL as one of the top 20 potential bacterial drug targets [12]. Although amphipaths that add tension to the membrane have been known to gate bacterial mechanosensitive channels [3,13,14], these are non-specific, also gating an unrelated bacterial mechanosensitive channel, MscS ('S' for smaller conductance).

We have performed a high-throughput screen (HTS) [15] and identified two novel MscL agonists, with antibiotic and adjuvant properties [16-18]. Given their different structures, they surprisingly bind in a similar binding pocket, at the cytoplasmic membrane interphase in a region of dynamic protein-protein and protein-lipid interactions that are crucial for MscL gating [19-21].

Citation: Lastname, F.; Lastname, F.; Lastname, F. Title. *Antibiotics* **2022**, *11*, x. https://doi.org/10.3390/xxxxx

Academic Editor: Firstname Lastname

Received: date
Accepted: date
Published: date

One major hurdle is identifying additional candidate MscL agonists, especially those with a novel scaffold, which will act as leads for potential drugs that maintain MscL agonist specificity have greater efficacy. Here, we have used an *in silico* screen for compounds that bind the same binding site, specifically looking for compounds not related to those previously characterized. We have found a new family of related compounds that specifically activate MscL as their sole mechanism of action, experimentally show all of the characteristics expected for agonists that bind to this region, but have a slightly different agonist character. These findings demonstrate that *in silico* screening is a viable approach for identifying and improving the design of novel MscL agonists.

2. Results

2.1. In silico screening: the identification and characterization of a small family of compounds that bind at the targeted location.

2.1.1. An in silico screen identifies a small family of related compounds from the ZINC library that are candidates for agonists for the *E. coli* MscL channel.

An *in silico* screen was performed with compounds from the ZINC library against the binding pocket previously found for the 011A and K05 MscL agonists. Promising hits were recognized according to their docking scores, and their agonist activities were confirmed by additional experimental approaches and more accurate molecular modeling techniques. We concentrated our efforts on "diverse" compounds not obviously related to those isolated previously. A small family of four related compounds appeared high on the list for having potential high affinity binding ZINC22855261, ZINC22409262, ZINC56952642, and ZINC22409190 (**Figure S1** shows structures of these and previously characterized compounds that bind to this site). We will refer to the ZINC compounds by their unique last three identifying numbers (261, 262, 642, and 190). All members of this family were characterized using MD simulations and *in vivo* growth and viability experiments. The binding free energy between each ligand with MscL was calculated using MM-PBSA-WSAS approach for 300 snapshots collected from a 150-nanosecond MD trajectory (See **Figures 1 and S2 to S4**). The compound 262 was the most stable during MD simulations and had the lower MM-PBSA-WSAS binding free energy, suggesting a higher affinity binding. Compound 262, with the lower binding affinity at -31.5 kcal/mol was followed by compounds 261, 642 and 190 (**Table S1**). Given these data, and the tractable nature of the molecule (see below), we concentrated our efforts studying compound 262.

2.1.2. Compound 262 decreases *E. coli* cell growth and viability in a MscL-dependent manner.

The compounds were then tested *in vivo* using whole-cell physiology. As predicted from the computational analyses, compound 262 decreased the growth and viability of bacterial cells in a MscL-dependent manner (**Figure 2**). In contrast, the expression of another bacterial mechanosensitive channel of a different family, MscS, did not make the strain susceptible to the 262 compound (**Figure 2A**). We found that compounds 261 and 642 also decreased cell growth in a MscL-specific manner (**Figure S7**). However, the 190 compound did not go into solution in 2% DMSO, demonstrating the limitations of the *in silico* screening approach and the necessity to complement this approach along with *in vivo* physiology. The ability of compound 262 to decrease growth and viability were similar to that previously observed for the compounds 011A and K05 [16-18]; compound 262 showed greater decreased growth relative to 011A at similar concentrations (**Figure S8**), confirming the potential advantage of the *in silico* screening approach.

The experimental data shown in **Figure 2** was performed in a MscL/MscS double-null strain with the channels, when expressed, expressed *in trans*. The expression construct used, pB10, is a mid-copy number plasmid that expresses MscL less than 10-fold greater than it is normally expressed endogenously [22]. However, even this relatively small increase in expression of only a few fold could have consequences in results

obtained. We therefore utilized strains selectively null for specific mechanosensitive channels and directly compared them to a strain expressing MscL *in trans*. As seen in **Figure 3**, two different concentrations of compound 262 were tested (20 and 40μM), and the effects were similar to those obtained with MscL *in trans*; MscL-specific affects were observed at wild-type endogenous levels.

2.1.3. MscL is sensitive to compound 262 in electrophysiological experiments.

We next tested if the 262 compound, like other agonists binding to the targeted site [16-18], increased the probability of opening (P_o) of the MscL channel when assayed by patch clamp of native membranes. As seen in **Figure 4,** MscL activity, measured in excised patches from giant spheroplasts [22], greatly increased with the addition of compound 262 in the bath chamber. A quantification of this effect is shown in **Figure 4B**; the probability of opening of MscL dramatically increases upon treatment with compound 262. Note that in excised patches all cytoplasmic proteins are removed, so the compound is exposed only to the membrane and membrane proteins. The fact that we found that the compound worked in the bath of the inside-out excised patch, which correlates with addition of the compound to the cytoplasmic side, is also consistent with the other agonists that diffuse across the membrane to obtain the binding site at the cytoplasmic-membrane interface (see **Figure 1**).

2.1.4. Compound 262 binds in the targeted pocket at the cytoplasmic/membrane and subunit interfaces.

Computational analyses of the binding of compound 262 to MscL were performed by MD simulations, leading to testable predictions by mutational analyses. The binding posture of the ligand and some of the potential interactions are shown in **Figure 5**; similar sites were found for the other compounds in the family (**Figure S2**)

MscL residues crucial for its interaction with compound 262 were further identified by MM-GBSA analysis (ΔG values less than -1.2, see **Table S2**). These residues include F10, A11, V17, I25, I232 (I96), N236 (N100), and F362 (F90). In agreement with these predictions, as shown in **Figure** 6, these residues, when mutated, lead to partial suppressors of the growth inhibition induced by compound 262 in WT MscL. Additionally, mutations of residues K97, L98 and I99, known to contribute to the binding of other ligands to this pocket [16-18], also all showed partial suppression. Hence, predictions from previous studies and computational analyses are supported by whole-cell physiological experiments.

Previously, to confirm binding sites, we have used orthologues that have differences in a proposed binding pocket. These orthologues show partial suppression of MscL-agonist-dependent slowed growth that is due to lower affinity binding. When the orthologues are modified to have the canonical binding site, an observed increase in agonist effectiveness gives strong evidence that the proposed site is indeed involved. In a general screen, we found that compound 262 was more effective against the *E. coli* MscL than that *Bacillus subtilis* (**Figure 7**).

The *B. subtilis* MscL channel differs in the canonical binding site for 011A and K05, other agonists that bind in this location, and the channel can be modified to become sensitive to the agonists by mutating the site to the canonical binding site [16-18]. The primary residue that differs is the binding site is K97, which is R in the analogous site in *B. subtilis* (R88). Consistent with previous results, we found that mutating this residue in *E. coli* to K97R led to a channel that did not respond well to compound 262 (**Figures 6 and 7**). More significantly, mutation of the analogous site in *B. subtilis* to the canonical site (R88K) leads to an increased sensitivity to compound 262 (**Figure 7A**). These data strongly support that the 262 compound is binding to this site of the MscL protein complex.

A second binding site, in the pore of the MscL channel, has been identified for dihydrostreptomycin. In previous studies, we have shown that this antibiotic binds to this site,

opens the MscL channel pore, and uses it as a pathway into the cytoplasm [23]. In this case, the canonical binding site is missing from the *H. influenza* orthologue, which can be mutated to make this orthologue sensitive to the antibiotic [23]. Although we found that *H. influenza* is not sensitive to compound 262, the mutation that makes MscL sensitive to dihydrostreptomycin does not make this homologue sensitive to compound 262 (**Figure 7B**), demonstrating specificity to the previously described binding site for 011A and K05.

Together the data are all consistent and confirm that compound 262 binds to the MscL channel in the pocked used for the *in silico* screen, demonstrating the power of this approach for MscL-targeted drug development.

2.1.5. Compound 262 works synergistically with kanamycin and other antibiotics.

Previous experiments have demonstrated that MscL agonists work in concert with several other antibiotics by allowing them passage into the cytoplasm [16,18,23]. As seen in **Figure 8**, at a sub-threshold concentration of Kanamycin, addition of compound 262 leads to a decreased growth much greater than either compound alone. Similar results were obtained for tetracycline (**Figure S9**). These data are consistent with those obtained for the other MscL agonists [16,18].

2.2. Figures

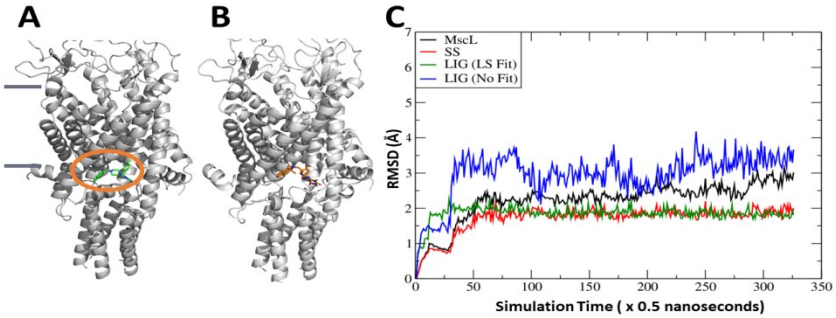

Figure 1. The binding site of compound 262 within the MscL structure as determined by docking and MD Simulations. **(**A) the docking pose of the compound, shown in green within the red circle at the cytoplasmic-membrane interface. The boundaries of the lipid bilayer are within the grey rectangles on the left. (B) Shown is a representative conformation of the ligand, in brown, within the pocket after MD Simulation. Note that it resides in the binding pocket with little conformational change. (C) Root-mean-square deviation (RMSD) analysis over time shows that compound 262 underwent some translational or rotational movement (blue curve), but the overall conformations are very similar to the docking pose. "MscL" (black curve) is for all residues, while "SS" (red curve) is for residues in secondary structures. The green and blue curves represent the RMSD of the ligand with and without least square fitting, respectively.

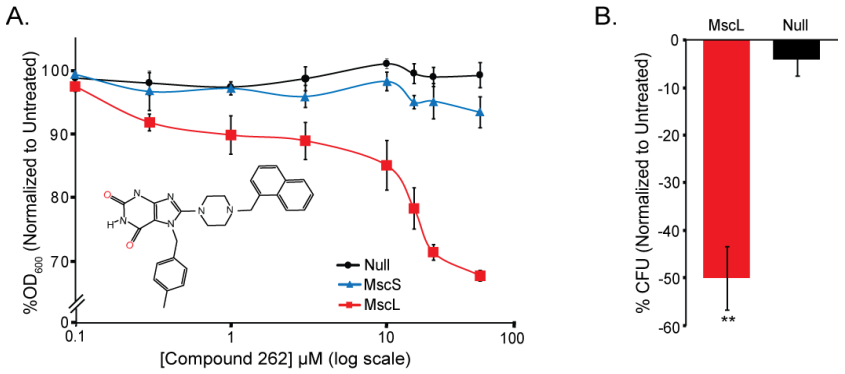

Figure 2. Compound 262 affects both growth and viability of *E. coli* cultures in a MscL dependent manner. *E. coli* MJF455 (ΔMscL, ΔMscS) bacterial strain are shown. For expression of MscL (red) and MscS (blue), the pb10d expression vector (black) was used. (A) Growth inhibition in the presence of increasing concentrations of compound 262 is shown as the percentage of growth (OD_{600}), normalized to untreated cultures. The structure of compound 262 is shown as an insert. (n=3) and error bars show standard error of the mean (SEM). (B) The percent reduction in CFU's normalized to untreated samples after overnight treatment with 40 µM compound 262 (n=4). ** $p<0.005$ by a 2-tailed, homoscedastic t-test.

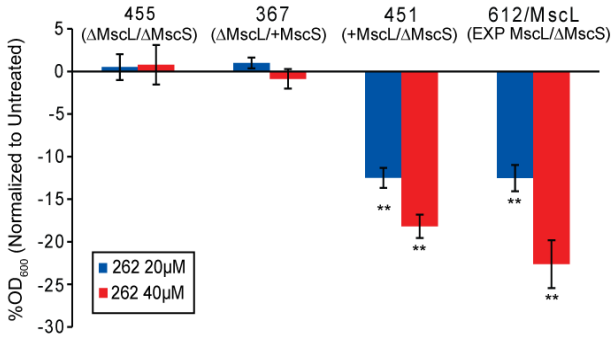

Figure 3. Compound 262 affects cultures with endogenous levels of expression of *E. coli* MscL. Cell lines used as indicated with endogenous levels of expression of MscL or MscL expressed *in trans* (EXP MscL), treated with compound 262 overnight at either 20μM (blue) or 40μM (red). Shown as the percent change in OD_{600} normalized to untreated cultures. (n=3) ** $p<0.005$ by a 2-tailed, homoscedastic t-test when compared to MJF455 (ΔMscL, ΔMscS) at the same concentration.

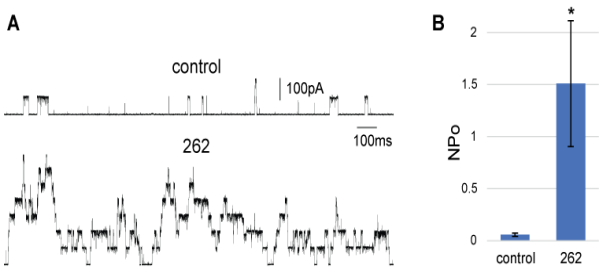

Figure 4. Compound 262 increases MscL activity in patch clamp of native bacterial membranes.

A) Representative traces of MscL activity in an excised patch from bacterial giant cells, held at a pressure of -110 mmHg, before (control) and after 10 minutes of the addition of 40 μM compound 262 to the bath. B) Quantification of MscL channel activity measured as the open probability (NPo) of the channels in a patch held at the same pressure, before and after curcumin treatment. * $p<0.05$ Student paired t-test, (n=5).

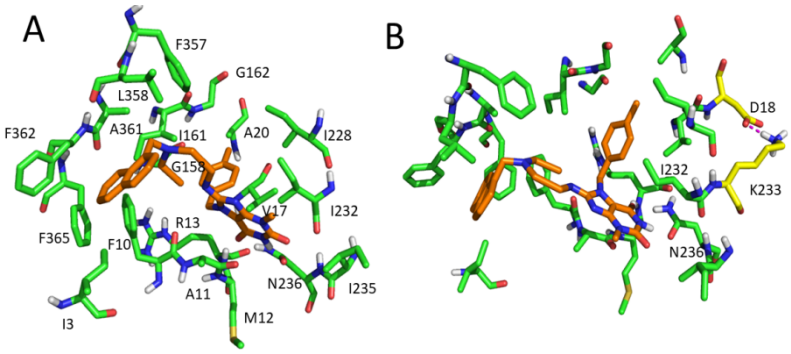

Figure 5. Two views of the 262 compound in the binding pocket after MD simulations; interactions with specific residues are shown.

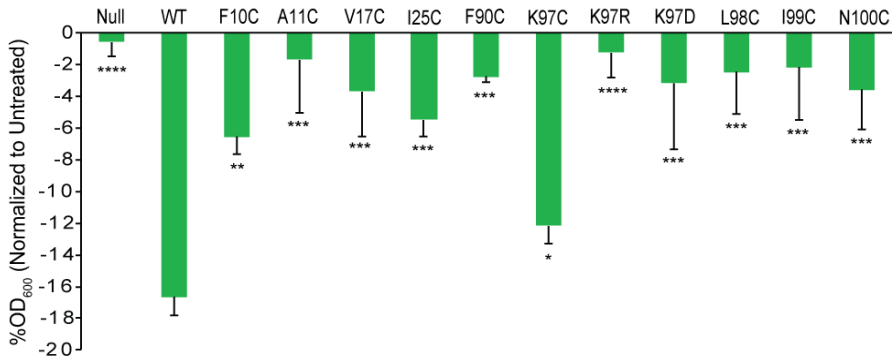

Figure 6. Mutational analysis provides additional evidence for the binding site of compound 262. Inhibition of growth after treatment of compound 262 at 40μM shown as OD_{600} normalized to untreated. MJF455 (ΔMscL, ΔMscS) cell line carrying pB10d empty plasmid (Null) or expressing, wild type *E. coli*-MscL (WT) or mutations of *E. coli*-MscL, as indicated. (n=3-10), *p<0.05, ** p<0.005, ***p<0.0005, ****p<0.00005, mutations vs. WT for either *E. coli*-MscL, 2-tailed, homoscedastic t-test.

181

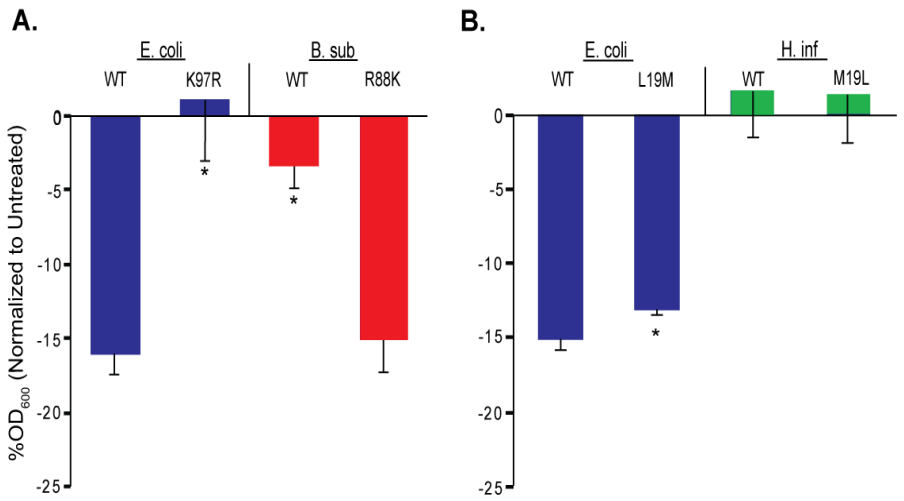

Figure 7. Compound 262 efficacies for cells espressing MscL orthologues and mutants of *Bacillus subtilis* and *Haemophilus influenzae* are consistent with its docking profile. *E. coli* strain MJF455 cultures, in the presence of 40μM compound 262. A) Note that changing the *E. coli*-MscL K97 to R decreases 262 sensitivity, whereas changing *B. sub*-MscL R88 to K increases sensitivity, consistent with the canonical sequence in the proposed binding pocket. B) *E. coli* expressing *E. coli*-MscL (E. coli) or the orthologue *Haemophilus influenzae* (H. inf). Note that changing the *E. coli*-MscL L19 to M or H. inf M19 to L does not change 262 sensitivity, demonstrating 262 does not share the canonical binding pocket in the pore, where dihydrostreptomycin is known to bind. (n = 3 to 6), * $p<0.05$, mutations vs. WT for either *E. coli- B.sub-* or *H. inf*-MscL, 2-tailed, homoscedastic t-test.

182

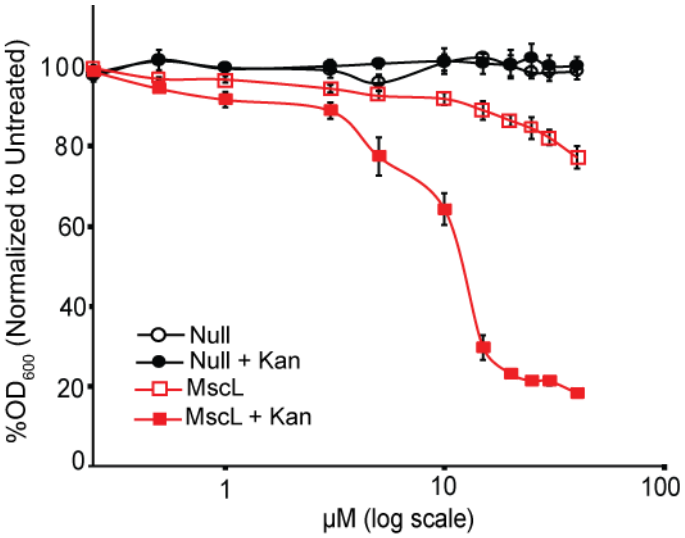

Figure 8. Compound 262 increases potency of the common antibiotic kanamycin only when MscL is present. Values are expressed as a percentage of growth (OD_{600}), relative to non-treated samples. MJF455 (ΔMscL, ΔMscS) cultures carrying empty plasmid (Null) or expressing *E. coli*-MscL (MscL), treated with varying concentrations of compound 262, grown in the presence or the absence of 0.5 μM kanamycin as indicated (n=3-4). error bars show standard error of the mean (SEM).

3. Discussion

Until the recent discovery of MscL specific agonists in an HTS screen, [15,16,18,23], only compounds with amphipathic properties were known to activate bacterial mechanosensitive channels. These compounds, like parabens and arachidonic acid, exert their unspecific effects mainly by altering the lipid membrane properties, to which many mechanosensitive channels proved sensitive (see [3] for a review).

Historically, one of the first chemical families used as topical antibiotics included dyes, some of which have been proposed to bind in the MscL pore [24]. An *in silico* screen to the region led to the discovery of "compound 10", coined as Ramizol [24]. However, Ramizol appears to have a second mechanism of action. It also affects MscS to some degree, demonstrating that it is not entirely specific because, like many amphipaths, it adds tension to the membrane. Finally, the evidence for Ramizol binding to the MscL pore is limited to docking studies by computational analysis and has not yet been demonstrated experimentally by mutational analysis.

The original HTS screen we performed found a handful of known antibiotics whose potency was increased with MscL expression [15]; the best characterized of these is dihydrostreptomycin, which has been shown by multiple approaches to directly bind to the pore of the MscL channel, activate it, and pass through it into the bacterial cell cytoplasm, thus increasing its potency [23]. The observation that a handful of antibiotics were found in the screen [15] suggests that drugs having MscL agonist properties as one of their mechanisms, or to get into the cell, may play a role in several systems. Indeed, we recently found that MscL is gated by curcumin, a natural antibiotic compound found in turmeric, and it is one of the two major mechanisms of the antibacterial properties this drug [25]. It thus seems possible, if not likely, that MscL may underlie other dual-mechanism drugs where one of the mechanisms is membrane permeation and/or loss of membrane potential (e.g. see [26]); further investigation in this area is necessary.

The original screen, in addition to known antibiotics, identified several candidates for novel MscL agonists. Interestingly, the first two characterized (011A and K05), although not obviously structurally related (see **Figure S1**), shared a similar binding site. It is of interest to note that the binding site is at a subunit interface, a common feature for ligand-gated channels first found for the muscle acetylcholine channel [27]; it is also at the cytoplasm/membrane interface. The site of this binding pocket was not initially suspected for playing a large energetic contribution for MscL gating because, unlike the pore, only a few mutations yielded gain-of-function phenotypes in random mutagenesis studies [8,10]. However, later, with the advance of our understanding of the functional role of N-terminal helix [28] and its interactions with the cytoplasmic regions of the TM domains [20], this region is now known to fine-tune the large structural changes required to open large-conducting MscL pore [20,21].

Here, with the use of *in silico* screening, combined with molecular dynamics (MD) simulations, we have successfully identified compounds that bind to this region that are new and distinct from those previously characterized, but sharing the property of MscL specificity. Interestingly, the family member best characterized in this manuscript, 262, was active in an HTS screen searching for compounds with antimicrobial activity against *M. tuberculosis* (PubChem AID 2842). This finding supports the notion that like 011A and K05, compound 262 will be effective against other pathogens. This compound 262 candidate was never followed-up or published for its activity on *M. tuberculosis*, presumably because the researchers were looking for compounds inhibiting a tuberculosis-specific kinase (as indicated in the text) – 262 simply did not hit the desired target. We have now determined the target is MscL.

Compound 262 has many similarities to 011A and K05, the other agonists that bind to the same pocket. It inhibits growth and has some cidal activity. It works at endogenous MscL expression levels. Electrophysiologically, it increases the probability of MscL channel opening in native membranes, even when the compound is added to the cytoplasmic side of the membrane. It also increases the potency of common antibiotics in a MscL-

dependent manner, suggesting that while members of this class of compounds may not serve as stand-alone antibiotics, they may evolve into efficient adjuvants. Several approaches confirmed that it binds the targeted binding pocket shared by 011A and K05, but its interactions with some specific residues yields a unique pattern. The diversity of the compounds that bind to this generalized site in unique ways bodes well for isolating compounds with increased potency and efficacy; indeed, 262 is better in these properties than the first and best characterized MscL agonist, 011A (see **Figure S4**). Thus, the findings presented here demonstrate that *in silico* screening is a viable approach for identifying novel MscL agonists with advantageous characteristics.

In silico screening can enrich two types of libraries, the diverse and focused screening libraries. The former is suitable to identify novel hits with different structures, while the latter can optimize the existing hits and facilitate to construct structure-activity relationships. Prior to compound acquisition and bioassays, the top hits can be validated with more rigorous molecular modeling methods, e.g., a promising ligand can stably reside in the binding pocket during the MD simulations, and has a decent binding affinity. Finally, the potency of the ligand is confirmed by bioassays. This approach was successfully applied here to identify promising activators of MscL using a gate-closed structure. However, there is a disadvantage of applying a closed MscL structure, i.e., one needs to run long MD simulations to conform if the ligand binding can trigger gate opening [18]. Also, physiologically, because the compounds only destabilize the closed state, the channel opening is transient and the efficacy *in vivo* is low. On the other hand, it is more promising to apply an open structure in the above *in silico* HTS protocol to identify potent binding compounds that can lock the MscL channel into an open state. The calculated binding affinity should reflect the ability of a ligand to maintain the MscL in the open state, and this ability can be evaluated through short MD simulations. Toward this end, we have collected a set of open state structures from MD simulations of the passage of dihydrostreptomycin and small proteins through the MscL channel [23]. In the future, utilizing established *in silico* HTS protocols on these open-channel structures should allow for the isolation of compounds that lock the channel in an open state, and thus have greatly increased efficacy in bacterial cidal activity.

~~section may be divided by subheadings. It should provide a concise and precise description of the experimental results, their interpretation, as well as the experimental conclusions that can be drawn.~~

4. Materials and Methods

4.1. Strains and Cell Growth.

The following bacterial *E. coli* Frag 1 derived strains were used as hosts in this study: MJF367 (ΔmscL::Cam), MJF451 (ΔMscS), MJF455 (ΔmscL::Cam, ΔMscS), and MJF612 (ΔmscL::cm, ΔmscS, ΔmscK::kan, ΔybdG::aprΔ) [11,29]. The pB10d expression vector was used alone or with constructs inserted for expression; note that this is a mid- level expression vector and expresses MscL at only a few times endogenous levels. Cultures inoculated from a single colony were grown either in citrate-phosphate-defined media (CphM) pH 7.0, consisting of per liter: 8.57 g of Na_2HPO_4, 0.87 g of K_2HPO_4, 1.34 g of citric acid, 1.0 g NH_4SO_4, 0.001 g of thiamine, 0.1 g of $MgSO_47H_2O$, 0.002 g of $(NH_4)2SO_4.FeSO_4.H_2O$, and incubated in a 37°C shaker, rotated at 250 cycles per minute.

4.2. In Vivo Assays

4.2.1. Growth experiments.

Growth inhibition was measured as previously described [15,23]. Briefly, overnight cultures of MJF376, MJF451, MJF455 or MJF612 strains carrying constructs, were diluted 1:50 in CphM and grown until an OD_{600} of 0.2 was reached. Expression was then induced by the addition of 1 mM isopropyl-b-D-thiogalactopyranoside (IPTG) for 30 minutes, 10 mM stocks of compound 262 solubilized in sterile dimethyl sulfoxide (DMSO) (Sigma,-

Aldrich, St. Louis, MO), was diluted to two times its final concentration in pre-warmed CphM with a final DMSO concentration of 2% and 100 µl was added to wells of a pre-warmed, sterile 96 well flat bottom plate (Greiner bio-one, Monroe, NC). Cultures were then diluted 1:200 in pre-warmed CphM, 100 µg/ml ampicillin and 2 mM IPTG with diluted experimental antibiotics, were indicated, at 2X their concentration or mock (DMSO only). Final concentrations of kanamycin A at 0.2 µM (Sigma Aldrich St. Louis, MO, CA) in 100 µl of culture mixture was added to the 96 will plates for a total of 200 µl, sealed with a sterile breathable film (Axygen, Union City, CA), wrapped in aluminum foil and placed in a 37°C shaker, rotated at 110 Cycles per minute for 16-17 hours and OD_{620} was then taken with a Multiskan Ascent 354 (Thermo Fisher Scientific Waltham, MA) plate reader.

4.2.2. Viability Experiments.

Cultures from the above overnight growth experiments were used for all viability experiments done as previously described [28]. Briefly, cultures were diluted 1:20 into pre-warmed CphM, serially diluted from 10^{-3} to 10^{-6} in a 96 well plate and liquid drops of 5 µl were placed on a pre-warmend LB ampicillin plates and placed in a 37°C incubator. The next morning colony-forming units were calculated to determine cell viability.

4.3. Electrophysiology

E. coli giant spheroplasts were generated and used for patch-clamp experiments as described previously (Blount 1999, trends microb). Excised, inside-out patches were examined at room temperature under symmetrical conditions using a buffer containing 200 mM KCl, 90 mM $MgCl_2$, 10 mM $CaCl_2$ and 5 mM HEPES pH 6 (Sigma, St. Louis, MO). To study the effects of compound 262, each patch was measured before and after 10 minutes of addition of the compound to the bath chamber, with the patch held at the same negative pressure. Recordings were performed at -20 mV (positive pipette). Data were acquired at a sampling rate of 20 kHz with a 5-kHz filter using an AxoPatch 200B amplifier in conjunction with Axoscope software (Axon Instruments, Union City, CA). A piezoelectric pressure transducer (World Precision Instruments, Sarasota, FL) was used to monitor the pressure throughout the experiments. Data were analyzed using Clampfit10 from pClamp10 software (Molecular Devices).

4.4. Molecular Modeling and Computational Analyses

4.4.1. *In silico* screenings.

We performed *in silico* docking screening using a subset of the ZINC database that we compiled [30]. Each compound in this subset has one or more structurally similar drug molecules (Tanimoto coefficient ≥ 0.85). All 123,192 compounds were ranked using the Glide [31] standard-precision docking scores. From this, 486 hits were identified using a docking score threshold of -9.5 kcal/mol. Then 100 diverse compounds were selected for potential further study. The Glide docking protocol was briefly described as follows: the binding site center was defined by a set of residues (I3, E6, F7, F10, I161, A361, F362, I364, F365 and K369) and the cubic binding site has a size length of 30 Å; the standard precision (SP) Glide was applied to evaluate docking poses with the intramolecular hydrogen bonds being rewarded; the planarity of the conjugated pi groups was enhanced during the docking simulations; for each compound, up to 100 docking poses were minimized in the post-docking minimization step and the best one was outputted. The same protocol was applied in our previous studies.[16-18]

4.4.2. Molecular dynamics simulations and free energy analysis.

Compounds that had activities were further studied using more rigorous molecular modeling techniques. MD simulations were performed to study binding stability and to collect representative conformations for free energy analysis. Each ligand-MscL system

contains one ligand, one MscL protein complex, 230 POPC lipids, 95 Cl-, 96 K+, and 32312 TIP3P water molecules. The force filed models that describe the systems include FF14SB [32] for proteins, GAFF2 [33] for ligands, and LIPID14 [34] for POPC, etc. The residue topologies of ligands were prepared using the Antechamber package [35]. Each system was first relaxed by a series of restrained minimizations with the harmonic restraint force constant applied to the main chain atoms decreased from decreased from 20 to 10, 5, and 1 kcal/mol/Å^2, progressively. The system was then fully optimized without any restraint for 5,000 steps. Next, 4-stage MD simulations were performed including the relaxation phase (four 100-picosecond MD simulations utilizing the same restraint scheme as minimizations), the system heating up phase (five 100-picsecond MD simulations with the desirable temperature being set to 50, 100, 150, 200 and 250 K), the equilibrium phase (298 K, 1 bar for 15 nanoseconds) and the final sampling phase (298 K, 1 bar for 150 nanoseconds). Integration of the equations of motion was conducted at a time step of 1 femtosecond (fs) for the first two phase and 2 fs for the last two phases. The root-mean-square deviations of main chain atoms (for MscL) and heavy atoms (for ligands) along MD simulation time were calculated to investigate the conformational changes upon ligand binding. Two types of RMSDs were calculated for a ligand, LS-Fit describes the conformational change of the ligand, while No-Fit also accounts for the translational and rotational movement of the ligand inside the binding pocket. No-Fit RMSDs were direct calculated after MD snapshots were aligned to the reference structure (the initial model of MscL) using only the secondary structures. The MD conformation which has the smallest RMSDs to the average structure of all the collected MD snapshots was identified as the representative MD conformation of a MD system. Besides the RMSD, we also evaluated the fluctuations of MscL and the overall size of the simulations system during MD simulations. The B-factors of individual residues and the radius of gyration (RoG) were shown in Figures S5 and S6, respectively. Overall, the B-factor and RoG data are reasonable and consistent with the RMSD result.

All 3000 snapshots sampled from the last phase were used to conduct MM-GBSA binding free energy decomposition analysis, while only 150 evenly selected snapshots were subjected to MM-PBSA-WSAS binding free energy calculation. For MM-GBSA free energy decomposition, the internal dielectric constant was set to 1, while the external dielectric constant was set to 2 for modeling the hydrophobic part of the POPC lipids. Unlike MM-GBSA free energy decomposition, we applied two external dielectrics (ε_{wat}=80 for water and ε_{lip}=2.0 for the lipid bilayer) in the MM-PBSA-WSAS binding free energy calculations. The membrane center offset parameter, mctrdz which is defined as the distance between the coordinate center of all phosphorous atoms and the coordinate center of MscL/ligand complex, and the thickness of membrane, mthick, which is defined as the distance between the coordinate centers of the phosphorous atoms in the upper and lower layers, varied from one MD snapshot to another. Thus, those two parameters were calculated for each individual snapshot. For a ligand itself, the implicit membrane option was turned off and the external dielectric constant was set to 80. The nonpolar part of a solvation free energy was calculated using the following equation: $\Delta G_{nonpolar} = 0.0054 \times SAS + 0.92$, where SAS is the solvent accessible surface area and 0.0054 is the surface tension coefficient parameter. The entropic term was estimated using the WSAS method described [36]. All the MD simulations and the followed free energy analysis were performed using the AMBER18 software package [37].

Supplementary Materials: The following supporting information can be downloaded at: www.mdpi.com/xxx/s1, Figure S1: Structures of MscL-specific agonists that bind within the same region of the channel; Figure S2: Computational analyses of compound 261; Figure S3: Computational analyses of compound 642; Figure S4: Computational analyses of compound 190; Figure S5: Residue-based B-Factor for the MD trajectories; Figure S6: The time courses of radius of gyration; Figure S7: Two closely related compounds also inhibit growth of *E. coli* cultures in a MscL dependent manner; Figure S8: Comparison of the effects of two MscL agonists on *E.coli* growth; Figure S9: Compound 262 can also increase the potency of the common antibiotic tetracycline when MscL is

present; Figure S1: title; Figure S1: title; Table S1: MM-PBSA-WSAS Binding Free Energy of the Identified activators of *E. coli* MscL Channel; Table S2: MM-GBSA Ligand-Residue Interaction Energies

Author Contributions: Conceptualization, I.I., J.W. and P.B.; methodology, R.W., P.B.; J.W. and I.I. formal analysis, R.W., P.B.; J.W. and I.I.; investigation, R.W., J.W. and I.I.; writing, R.W., P.B.; J.W. and I.I.; funding acquisition, P.B. and J.W. All authors have read and agreed to the published version of the manuscript.

Funding: This research was funded by Grants I-1420 of the Welch Foundation, GM121780 from the National Institutes of Health (NIH), and 1955260 from the National Science Foundation (NSF).

Data Availability Statement: Not applicable

Acknowledgments: The authors also thank the Center for Research Computing (CRC) at University of Pittsburgh for the computing resources provided. The funders had no role in study design, data collection, analysis, decision to publish, or manuscript preparation.

Conflicts of Interest: The authors declare no conflict of interest. The funders had no role in the design of the study; in the collection, analyses, or interpretation of data; in the writing of the manuscript, or in the decision to publish the results".

5. Conclusions

This section is not mandatory but can be added to the manuscript if the discussion is unusually long or complex.

References

1. Booth, I.R.; Blount, P. The MscS and MscL families of mechanosensitive channels act as microbial emergency release valves. *J Bacteriol* **2012**, *194*, 4802-4809.
2. Cox, C.D.; Bavi, N.; Martinac, B. Bacterial Mechanosensors. *Annual Review of Physiology* **2018**, *80*, 71-93, doi:10.1146/annurev-physiol-021317-121351.
3. Blount, P.; Iscla, I. Life with Bacterial Mechanosensitive Channels, from Discovery to Physiology to Pharmacological Target. *Microbiol Mol Biol Rev* **2020**, *84*.
4. Levina, N.; Totemeyer, S.; Stokes, N.R.; Louis, P.; Jones, M.A.; Booth, I.R. Protection of *Escherichia coli* cells against extreme turgor by activation of MscS and MscL mechanosensitive channels: identification of genes required for MscS activity. *EMBO Journal* **1999**, *18*, 1730-1737.
5. Cruickshank, C.C.; Minchin, R.F.; Le Dain, A.C.; Martinac, B. Estimation of the pore size of the large-conductance mechanosensitive ion channel of *Escherichia coli*. *Biophysical Journal* **1997**, *73*, 1925-1931.
6. Perozo, E.; Cortes, D.M.; Sompornpisut, P.; Kloda, A.; Martinac, B. Open channel structure of MscL and the gating mechanism of mechanosensitive channels. *Nature* **2002**, *418*, 942-948.
7. Poolman, B.; Blount, P.; Folgering, J.H.; Friesen, R.H.; Moe, P.C.; van der Heide, T. How do membrane proteins sense water stress? *Molecular Microbiology* **2002**, *44*, 889-902.
8. Maurer, J.A.; Dougherty, D.A. A high-throughput screen for MscL channel activity and mutational phenotyping. *Biochimica et Biophysica Acta* **2001**, *1514*, 165-169.
9. Iscla, I.; Wray, R.; Eaton, C.; Blount, P. Scanning MscL Channels with Targeted Post-Translational Modifications for Functional Alterations. *PLoS One* **2015**, *10*.
10. Ou, X.; Blount, P.; Hoffman, R.J.; Kung, C. One face of a transmembrane helix is crucial in mechanosensitive channel gating. *Proceedings of the National Academy of Sciences of the United States of America* **1998**, *95*, 11471-11475.
11. Levin, G.; Blount, P. Cysteine scanning of MscL transmembrane domains reveals residues critical for mechanosensitive channel gating. *Biophys J* **2004**, *86*, 2862-2870.

12. Barh, D.; Jain, N.; Tiwari, S.; Parida, B.P.; D'Afonseca, V.; Li, L.; Ali, A.; Santos, A.R.; Guimarães, L.C.; de Castro Soares, S.; et al. A novel comparative genomics analysis for common drug and vaccine targets in Corynebacterium pseudotuberculosis and other CMN group of human pathogens. *Chem Biol Drug Des* **2011**, *78*, 73-84.
13. Martinac, B.; Adler, J.; Kung, C. Mechanosensitive ion channels of *E. coli* activated by amphipaths. *Nature* **1990**, *348*, 261-263.
14. Perozo, E.; Kloda, A.; Cortes, D.M.; Martinac, B. Physical principles underlying the transduction of bilayer deformation forces during mechanosensitive channel gating. *Nature Structural Biology* **2002**, *9*, 696-703.
15. Iscla, I.; Wray, R.; Wei, S.; Posner, B.; Blount, P. Streptomycin potency is dependent on MscL channel expression. *Nature communications* **2014**, *5*, 4891, doi:10.1038/ncomms5891.
16. Wray, R.; Herrera, N.; Iscla, I.; Wang, J.; Blount, P. An agonist of the MscL channel affects multiple bacterial species and increases membrane permeability and potency of common antibiotics. *Mol Microbiol* **2019**, *112*, 896-905.
17. Wray, R.; Iscla, I.; Kovacs, Z.; Wang, J.; Blount, P. Novel compounds that specifically bind and modulate MscL: insights into channel gating mechanisms. *Faseb J* **2019**, *33*, 3180-3189.
18. Wray, R.; Wang, J.; Iscla, I.; Blount, P. Novel MscL agonists that allow multiple antibiotics cytoplasmic access activate the channel through a common binding site. *PLoS One* **2020**, *15*.
19. Iscla, I.; Wray, R.; Blount, P. An *in vivo* screen reveals protein-lipid interactions crucial for gating a mechanosensitive channel. *Faseb J* **2011**, *25*, 694-702.
20. Iscla, I.; Wray, R.; Blount, P. The dynamics of protein-protein interactions between domains of MscL at the cytoplasmic-lipid interface. *Channels* **2012**, *6*, 255-261.
21. Li, J.; Guo, J.; Ou, X.; Zhang, M.; Li, Y.; Liu, Z. Mechanical coupling of the multiple structural elements of the large-conductance mechanosensitive channel during expansion. *Proc Natl Acad Sci U S A* **2015**, *112*, 10726-10731.
22. Blount, P.; Sukharev, S.I.; Moe, P.C.; Martinac, B.; Kung, C. Mechanosensitive channels of bacteria. In *Methods in Enzymology*, Conn, P.M., Ed.Conn, P.M., Ed.; Ion Channels, Part C; Academic Press: San Diego, CA, 1999; Volume 294, pp. 458-482.
23. Wray, R.; Iscla, I.; Gao, Y.; Li, H.; Wang, J.; Blount, P. Dihydrostreptomycin Directly Binds to, Modulates, and Passes through the MscL Channel Pore. *PLoS Biol* **2016**, *14*, e1002473, doi:10.1371/journal.pbio.1002473.
24. Iscla, I.; Wray, R.; Blount, P.; Larkins-Ford, J.; Conery, A.L.; Ausubel, F.M.; Ramu, S.; Kavanagh, A.; Huang, J.X.; Blaskovich, M.A.; et al. A new antibiotic with potent activity targets MscL. *J Antibiot* **2015**, *68*, 453-462.
25. Wray, R.; Iscla, I.; Blount, P. Curcumin activation of a bacterial mechanosensitive channel underlies its membrane permeability and adjuvant properties. *PLoS Pathog* **2021**, *17*, e1010198, doi:10.1371/journal.ppat.1010198.
26. Martin, J.K., 2nd; Sheehan, J.P.; Bratton, B.P.; Moore, G.M.; Mateus, A.; Li, S.H.; Kim, H.; Rabinowitz, J.D.; Typas, A.; Savitski, M.M.; et al. A Dual-Mechanism Antibiotic Kills Gram-Negative Bacteria and Avoids Drug Resistance. *Cell* **2020**, *181*, 1518-1532 e1514.
27. Blount, P.; Merlie, J.P. Molecular basis of the two nonequivalent ligand binding sites of the muscle nicotinic acetylcholine receptor. *Neuron* **1989**, *3*, 349-357.
28. Iscla, I.; Wray, R.; Blount, P. On the structure of the N-terminal domain of the MscL channel: helical bundle or membrane interface. *Biophys J* **2008**, *95*, 2283-2291.
29. Schumann, U.; Edwards, M.D.; Rasmussen, T.; Bartlett, W.; van West, P.; Booth, I.R. YbdG in Escherichia coli is a threshold-setting mechanosensitive channel with MscM activity. *Proc Natl Acad Sci U S A* **2010**, *107*, 12664-12669.
30. Wang, J.; Ge, Y.; Xie, X.Q. Development and Testing of Druglike Screening Libraries. *J Chem Inf Model* **2019**, *59*, 53-65, doi:10.1021/acs.jcim.8b00537.
31. Friesner, R.A.; Banks, J.L.; Murphy, R.B.; Halgren, T.A.; Klicic, J.J.; Mainz, D.T.; Repasky, M.P.; Knoll, E.H.; Shelley, M.; Perry, J.K.; et al. Glide: a new approach for rapid, accurate docking and scoring. 1. Method and assessment of docking accuracy. *J Med Chem* **2004**, *47*, 1739-1749, doi:10.1021/jm0306430.
32. Maier, J.A.; Martinez, C.; Kasavajhala, K.; Wickstrom, L.; Hauser, K.E.; Simmerling, C. ff14SB: Improving the Accuracy of Protein Side Chain and Backbone Parameters from ff99SB. *J Chem Theory Comput* **2015**, *11*, 3696-3713, doi:10.1021/acs.jctc.5b00255.
33. Wang, J.; Wolf, R.M.; Caldwell, J.W.; Kollman, P.A.; Case, D.A. Development and testing of a general amber force field. *J Comput Chem* **2004**, *25*, 1157-1174, doi:10.1002/jcc.20035.

34. Dickson, C.J.; Madej, B.D.; Skjevik, A.A.; Betz, R.M.; Teigen, K.; Gould, I.R.; Walker, R.C. Lipid14: The Amber Lipid Force Field. *J Chem Theory Comput* **2014**, *10*, 865-879, doi:10.1021/ct4010307.
35. Wang, J.; Wang, W.; Kollman, P.A.; Case, D.A. Automatic atom type and bond type perception in molecular mechanical calculations. *J Mol Graph Model* **2006**, *25*, 247-260.
36. Wang, J.; Hou, T. Develop and test a solvent accessible surface area-based model in conformational entropy calculations. *J Chem Inf Model* **2012**, *52*, 1199-1212, doi:10.1021/ci300064d.
37. Case, D.A.; Berryman, J.T.; Betz, R.M.; Cerutti, D.S.; Cheatham, I.; T.E.; Darden, T.A.; Duke, R.E.; Giese, T.J.; Gohlke, H.; et al. Amber 14. **2014**.